



Spectrally combined three-diode-pumped compact femtosecond Ti:sapphire laser exceeding 1 W mode-locked power

DONG HOON SONG* AND HONG-SEOK SEO

Welfare & Medical ICT Research Department, Intelligent Convergence Research Laboratory, Electronics and Telecommunications Research Institute, Daejeon 34129, Republic of Korea

*dhsong@etri.re.kr

Abstract: The achievement of a high average power exceeding 1 W remains a major challenge for direct-diode pumped and mode-locked femtosecond Ti:sapphire lasers. Herein, we demonstrate high-power soliton-like pulses from a direct spectrally combined three-diode-pumped and semiconductor saturable absorber mirror (SESAM)-based mode-locked Ti:sapphire laser. Its mode-locked output power of up to 1 W was obtained in correspondence with a 68.8 MHz repetition rate and 55 fs pulse duration; thus, the pulse energy and peak power are 14.5 nJ and 264 kW, respectively. To the best of our knowledge, this is the highest reported output power and pulse energy from a Ti:sapphire laser with three spectrally combined pump diodes (471 nm, 491 nm, and 525 nm) and a simple beam expander. For efficient pumping, the combined pump beam, directed into the lens ($f = 60$ mm), which comprised three aspheric lenses along the fast axis and a shared cylindrical beam telescope ($8\times$ magnification) along the slow axis, resulting in a circular-focused beam in the Ti:sapphire crystal. The beam waist was measured to be $39\ \mu\text{m} \times 38\ \mu\text{m}$ along the slow and fast axes.

© 2021 Optical Society of America under the terms of the [OSA Open Access Publishing Agreement](#)

1. Introduction

Since the discovery of Ti:sapphire (Ti:S) crystals with broad gain bandwidths [1], femtosecond solid-state lasers made of Ti:S have become key technologies in a wide variety of applications in industry and basic science, such as precise machining, bioimaging, ophthalmic surgery, and ultrafast science [2–6]. Owing to their relatively weak absorptions in the blue–green wavelength region and short fluorescence lifetimes ($3.2\ \mu\text{s}$), Ti:S femtosecond lasers are predominantly pumped using frequency-doubled diode-pumped solid-state lasers (DPSSLs) with high beam quality; however, they are expensive, highly complex, and bulky [7,8]. Thus, there is a limit to their wider use.

With the major advancements in high-power laser diodes (LDs) in the spectral blue–green region, a direct-diode-pumped blue (452 nm) Ti:S femtosecond laser using a prism pair and a saturable Bragg reflector (SBR) to generate an output power of 13 mW and pulse duration of 114 fs at a repetition rate of 127 MHz was reported [9]. In a subsequent work, these researchers achieved an output power of 101 mW and pulse duration of 111 fs with both-way pumping [10]. Around the same time, a Kerr-lens mode-locked (ML) Ti:S femtosecond laser generating an output power of 34 mW and pulse duration of 15 fs was demonstrated using two blue diodes [11]. These works heralded simple, robust, and ultralow-cost Ti:S femtosecond lasers. Till date, femtosecond lasers with high average power outputs have been realized by several groups. Gurel et al. demonstrated 450 mW, 58 fs, 1.1 nJ pulses at 400 MHz by Kerr-lens mode-locking (KLM) as well as 200 mW, 68 fs, 0.5 nJ pulses by SESAM mode-locking [12]. Backus et al. have also reported 145 mW, 13 fs, 1.85 nJ pulses using single-laser diode pumping and 350 mW, < 20 fs, 4.5 nJ pulses using three spectrally combined blue pump diodes [13]. However, all these works could not avoid the formation of a focused elliptical spot in the gain crystal owing to different M^2

values along the fast and slow axes and the use of one cylindrical lens telescope for each diode [9–14]. Thus, for efficient pumping, a circular beam focused in the gain crystal with increased power and energy scaling is crucial.

Herein, we present a new and simpler technique to increase the ML average power and pulse energy by exploiting three spectrally combined pump diodes with blue (471 nm), sky-blue (491 nm), and green (525 nm) colors. The beams were combined using two dichroic filters as well as directed on and focused in a Ti:S crystal using a planoconvex lens and a simple beam expander; the beam expander comprised three aspheric lenses for each of the diodes for fast-axis beam collimation and a shared cylindrical telescope for slow axis beam collimation. The focused beam diameter without considering the Brewster angle of the Ti:S crystal was measured to be $78 \mu\text{m}$ along the slow axis and $76 \mu\text{m}$ along the fast axis directions owing to the different M^2 values of each diode, which is described in detail later. Thus, we experimentally obtained self-started femtosecond pulses with $> 1 \text{ W}$ ML power and 55 fs pulse duration at 68.8 MHz repetition rate in a negative dispersion regime. This enables high output power from the diode-pumped femtosecond Ti:S lasers.

2. Experimental methods

The experimental setup used in this work is depicted in Fig. 1(a). The laser cavity has a standard

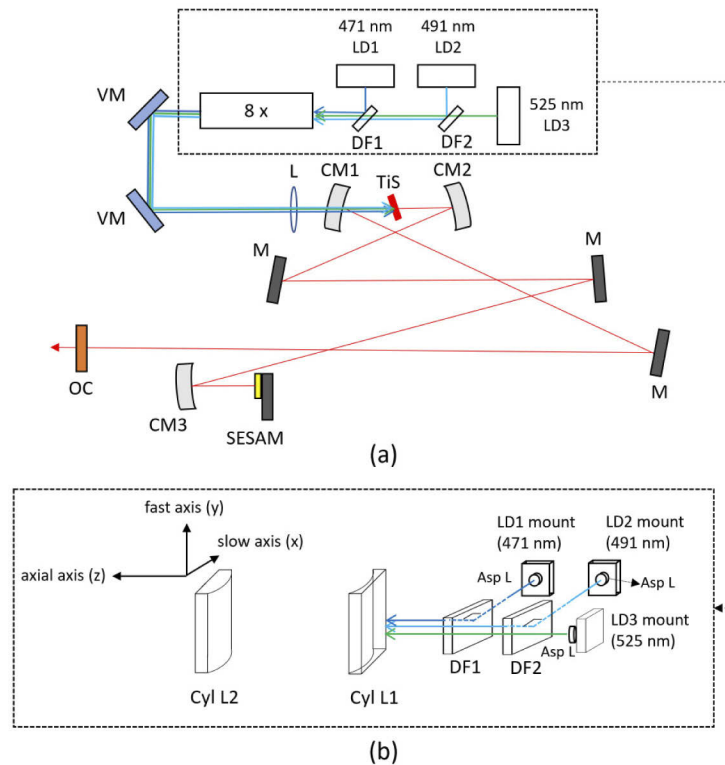


Fig. 1. (a) Experimental setup of the femtosecond laser. LDs, laser diodes; DFs, dichroic filters; VMs, visible flat mirrors; L, lens, CMs, dichroic curved mirrors; Ti:S, Ti:sapphire crystal; Ms, flat mirrors; CM3, curved mirror; OC, output coupler, (b) pump module consisting of three aspheric lenses (Asp L), two dichroic filters (DF1 and DF2), and the cylindrical telescope (Cyl L1 and Cyl L2)

X-fold configuration and consists of several flat chirped mirrors (M) generating negative group-delay dispersion (GDD), concave dichroic pump mirrors (CM1 & CM2) of radius of curvature 10 cm, a Ti:S crystal, a concave mirror (CM3) with radius of curvature 15 cm for a SESAM, and an output coupler (OC) with 5% transmission. The CM1 exhibited a high transmission ($T > 97\%$) at 450–550 nm as well as a high reflectivity ($R > 99.9\%$) at 710–890 nm. The cavity has a short arm of 876 mm (CM1 ~ OC) and a long arm of 1195 mm (CM2 ~ SESAM). Thus, the overall length of the cavity is 2.18 m, which corresponds to a repetition rate of 68.8 MHz. The Ti:S crystal (GT Advanced Technologies) of length 6 mm, Brewster-cut with an absorption coefficient of 2.71 /cm at 532 nm, figure-of-merit (FOM) of 150, and water-cooled on a copper mount, was placed between the two pump mirrors (CM1 & CM2). The intracavity net GDD of about -200 fs^2 allowed SESAM mode-locking operation.

For self-started passive mode-locking with advantages over the KLM, a SESAM (Reflekron) characterized by a low-intensity reflectance of 98% and high reflective band from 770 nm to 830 nm was placed in front of CM3. In addition, it has a saturation fluence of $60 \mu\text{J}/\text{cm}^2$, relaxation time of 5 ps, and nonsaturable loss of $< 0.5\%$. The beam waist on the SESAM in the cavity was designed to be $\sim 80 \mu\text{m}$, which corresponded to ~ 5 times the saturation fluence. Once the SESAM became slow saturable absorber, soliton-like pulses were stably generated; further details are given in Ref. [15–18].

As shown in Fig. 2(b), the three combined diodes (Nichia Corporation) operating at 471 (blue), 491 (sky blue), and 525 nm (green) were used as the pumping sources, which contained three aspheric lenses ($f = 4 \text{ mm}$, $\text{NA} = 0.6$) to collimate each diode beam along the fast axis, and an $8\times$ cylindrical telescope ($f = -25 \text{ (Cyl L1)}$ and 200 mm (Cyl L2)) to collimate the combined beam along the slow axis. The telescope with the aperture of the 20 mm (slow axis) and 30 mm (fast axis), respectively was utilized. The pumping sources were spectrally and coaxially combined by dichroic filters (DF1 and DF2, incident angle: 45°); these diodes were water-cooled on an aluminum mount at a temperature of 17°C , which was also linked to the Ti:S crystal. The

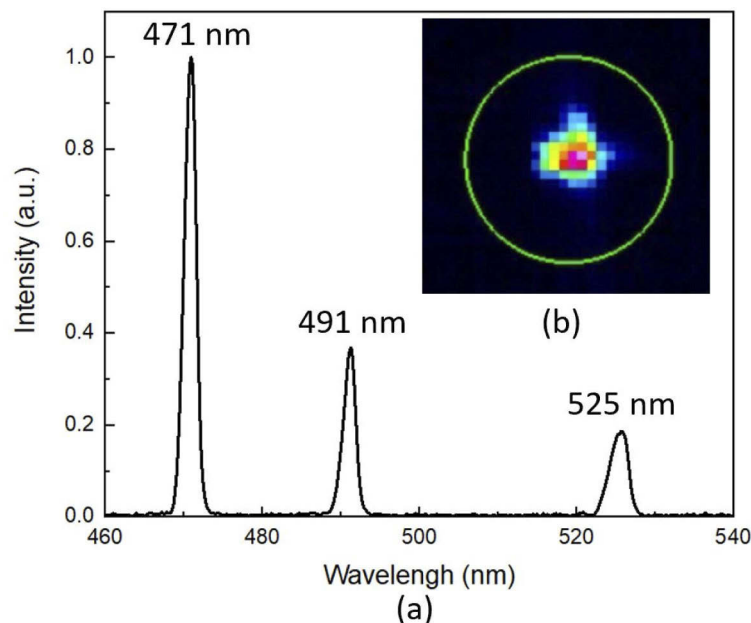


Fig. 2. (a) Spectrum of the combined pump beam, and (b) inset: focused beam profile with a lens of $f = 60 \text{ mm}$ measured to be $39 \mu\text{m}$ (slow axis) \times $38 \mu\text{m}$ (fast axis) μm at the beam waist.

three diodes emitted output powers of 6.1, 2.5, and 1.4 W, corresponding to low over-driven currents (4.3, 2.4, and 2.6 A for the 471, 491, and 525 nm LDs, respectively), and resulted in M^2 values (measured using a Thorlabs BP209) of 10.2×1.5 , 6.0×1.8 , and 4.6×2.3 , respectively, along the slow and fast axes. The M^2 value for the combined beam with an assumed wavelength of 471 nm, was measured to be 12.1×3.6 . A power meter (Gentec-EO, UP19K-30H-W5-D0) was installed in front of the anti-reflection-coated lens (L), as shown in Fig. 1(a), and the total output power of the combined beam was measured to exceed 9 W. The pump module consisting of three aspheric lenses, two dichroic filters, and one cylindrical telescope, as shown in Fig. 2(b), exhibited a transmission of 90%. No degradations were observed over 48 h. The combined beam was directed on the Ti:S crystal through a planoconvex lens ($f = 60$ mm). The single-pass power absorption of the Ti:S Brewster-cut crystal was measured to be 85.3% for 9.0 W pumping with the combined beam. This result is further discussed in the next section.

3. Results and discussion

First, a high pump power of over 9 W was obtained by combining the three pump diodes. For efficient pumping in the Ti:S crystal, a tight focus of the combined beam of less than $50 \mu\text{m}$ beam waist is generally necessary. However, owing to the different M^2 values along the slow and fast axes of the three diodes, the focused beam waists of the three diodes through CM1 were measured as 30×10 (471 nm LD), 38×14 (491 nm LD), and $48 \times 18 \mu\text{m}^2$ (525 nm LD). Furthermore, owing to the different M^2 values, the focused combined beam waist through CM1 was $39 \mu\text{m} \times 38 \mu\text{m}$ at the particular position, shown in Fig. 2(b), indicating that it appeared almost circular. To clarify the beam shape, we measured the relative positions of the foci of the combined beam as well as of the individual beams emitted by each diode. When the focus of the combined beam at the slow axis was assumed to be at the zero position, the corresponding focus at the fast axis appeared at a distance of +0.8 mm in the axial direction. The positions of the foci at the slow and fast axes for the 471 nm LD, 491 nm LD, and 525 nm LD beams were found to be (0, +0.5 mm, +0.2 mm) and (+0.5 mm, +1.5 mm, +1.3 mm), respectively, relative to the position of the combined-beam focus at the slow axis. The position of the circular-combined-beam focus was coincident with that of the 471 nm LD beam at the slow axis. In addition, we measured the circularity (expressed as: beam diameter (fast axis)/beam diameter (slow axis)) of the beam which evolved over half length of the crystal (6 mm) on either side of this circular point, as 0.73, 0.74, 0.73, 0.67, 0.78, 0.80, 0.97, 0.57, 0.43, 0.32, 0.41, 0.50, and 0.53 with a distance interval of 0.5 mm. Although the pump-beam waist measurement did not consider the Brewster angle, the data shows the feasibility of high pumping efficiency equal to that of the DPSSL, resulting in high slope efficiency as shown in Fig. 3.

Second, we initially pumped the Ti:S crystal using the 471 nm LD and later added either the 491 nm or 525 nm LD or both pumps. Figure 3(a) shows the ML output power versus the 471 nm LD pump power. Self-mode-locking was achieved without any contact soon as the continuous wave was lased over 7 mW at 2.6 W pumping of the 471 nm LD. Thereafter, the ML pulses were stably maintained, and the average power increased to 386 mW at 6.0 W pump power of the 471 nm LD, which is the power limit of the LD. The slope efficiency in this case was 11%. The laser cavity was aligned well at the pumping powers of all three LDs. Figures 3(b), 3(c), and 3(d) show the variations in the ML output powers as functions of different LD pump powers. At 5.8 W pump power of the 471 nm LD, the ML output powers were measured by adding either the 491 nm LD, or 525 nm LD, or both. As a function of the additional 491 nm LD pump power, the ML output power (black curve) increased from 372 to 728 mW for a slope efficiency of 14.5% (Fig. 3(b)). Sequentially, as a function of the added 525 nm LD pump power, the ML output power (red curve) increased from 372 to 533 mW with a slope efficiency of 13.7%. As a function of adding both the 491 & 525 nm LD pump powers, the ML output (blue curve) increased from 372 to 876 mW with a slope efficiency of 13.9%, as shown in Fig. 3(b). Here, when both LD

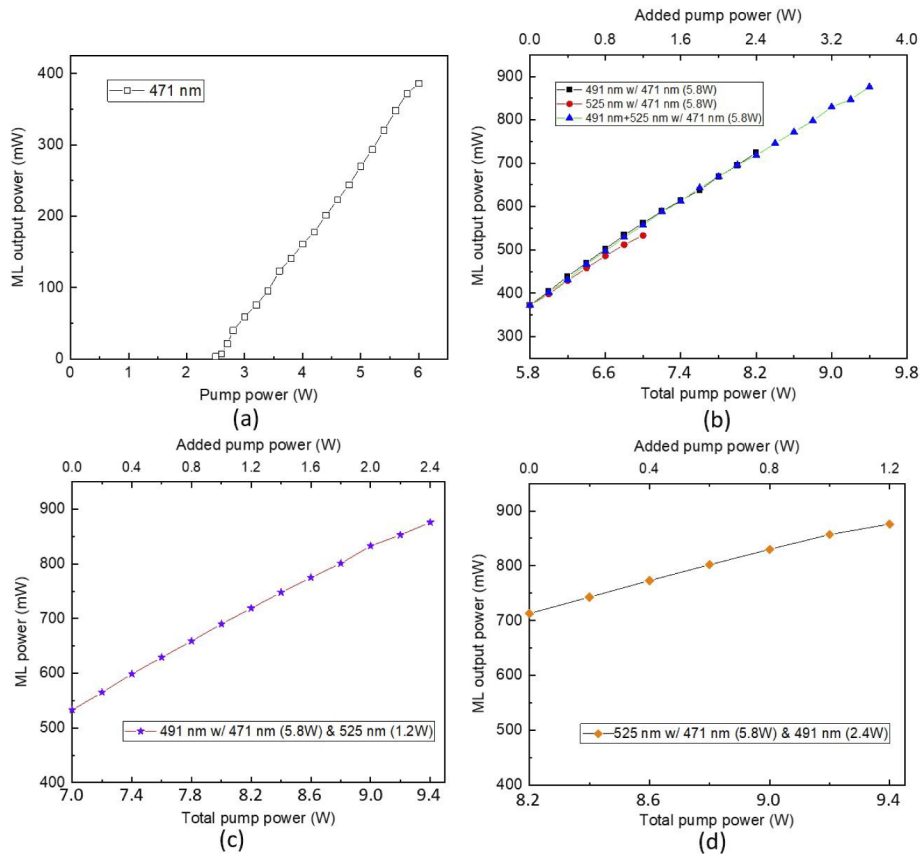


Fig. 3. Mode-locked (ML) output power performance of the combined pump beam. ML output power with (a) only 471 nm LD pump power; (b) 5.8 W power of the 471 nm LD pump and co-pumping with additional pump power of the 491 nm (black line), 525 nm (red line), and both 491 & 525 nm (blue line) LDs; (c) 5.8 W (471 nm) and 1.2 W (525 nm) LD pumping in addition to co-pumping with 491 nm LD (pink star line); (d) 5.8 W (471 nm) and 2.4 W (491 nm) in addition to co-pumping with the 525 nm LD (orange diamond line).

pumps were added, the power increased by up to 2.4 W (0.5 (491 nm)+0.5 (525 nm) = 1 W, 1.0 (491 nm)+1.0 (525 nm) = 2 W, 1.2 (491 nm)+1.2 (525 nm) = 2.4 W) until the power limit of the 525 nm LD. Thereafter, the power increased only by pumping with the 491 nm LD. As shown in Fig. 3(c), when using both 5.8 W of the 471 nm LD and 1.2 W of the 525 nm LD pumps as a function of the additional 491 nm LD pump power, the ML output power gradually increased from 533 to 876 mW with a slope efficiency of 14.4%. When using both 5.8 W of the 471 nm and 2.4 W of the 491 nm LD pumps as a function of the additional 525 nm LD pump power, the ML output power increased from 713 to 876 mW with a slope efficiency of 13.8% (Fig. 3(d)). Thus, all slope efficiencies were estimated to be similar at $\sim 14\%$, which was higher than that with 471 nm LD pumping only. These results ensure high optical efficiency performance.

The temporal response of the ML output power was investigated with the three pump LDs, as shown in Fig. 4(a). Figure 4(b) shows the enlarged timescale. For pumping applied in the sequence 471-525-491 nm (red line) and 471-491-525 nm (black line), the power was accumulated and switched repeatedly, with a sampling rate of 1 Hz. Although the Ti:S crystal with low FOM (150) was used as the gain medium, there were no large pump-induced losses, as noted in Ref. [19,20]. A slight transient pump-induced loss was observed for the LD pump switching;

however, the ML output power stabilized within 1 min because the charge transfer interactions in $Ti^{3+}-Ti^{4+}$ pairs quickly achieved steady states while the femtosecond pulses were reflected within the cavity. After optimizing the maximum power extraction at the highest pump powers of the three LDs (6.0 W of 471 nm, 2.4 W of 491 nm, and 1.2 W of 525 nm), the ML output power and stability were measured over 12 h, as shown in Fig. 5. The average ML output power was 1 W (maximum of 1040 mW), and the root-mean-squared stability was less than 1.2%, resulting in an optical-to-optical efficiency of 10.8%. This is the highest observed, reliable ML output power generated from a Ti:S laser. No degradation of the ML output power was observed over 12 h since the early self-ML.

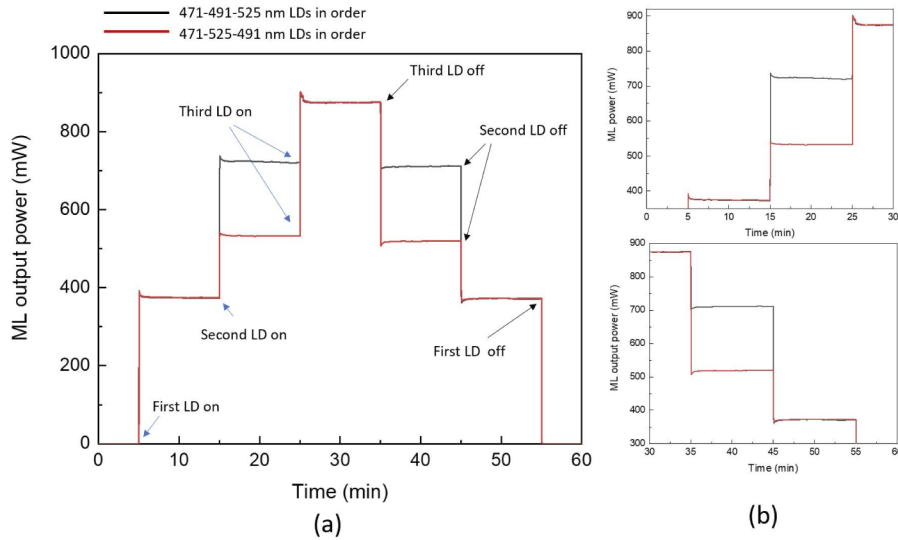


Fig. 4. Mode-locked output power responses as functions of time for the (a) combined pump beam and its (b) enlarged views.

Finally, to verify stable femtosecond pulse generation, the ML output spectrum, pulse durations, optical pulse trains, M^2 values, and beam profiles were measured. As shown in Fig. 6, the laser output spectrum had a bandwidth of 13 nm full-width at half maximum (FWHM) at a central wavelength of 798 nm. Further, the corresponding pulse durations were characterized using a commercial autocorrelator (MiniPD, APE GmbH), which revealed a pulse duration of 85 fs FWHM resulting in a 55 fs FWHM assuming a sech^2 intensity profile. An ML pulse train of period 14.5 ns was observed corresponding to the laser repetition rate of 68.8 MHz. The beam quality of the M^2 value was measured as 1.02×1.01 along the x & y axes, which is close to the ideal value of 1.0 (Fig. 6(d)). The beam profile, measured 1 m away from the laser head, is shown in Fig. 6(e), corresponding to a beam diameter of 2.4 mm. These evaluations ensure the feasibility of high-power exceeding 1 W with a standard Ti:S laser cavity configuration based on a simple beam expander comprising three spectrally combined pump diodes (471 nm, 491 nm, and 525 nm).

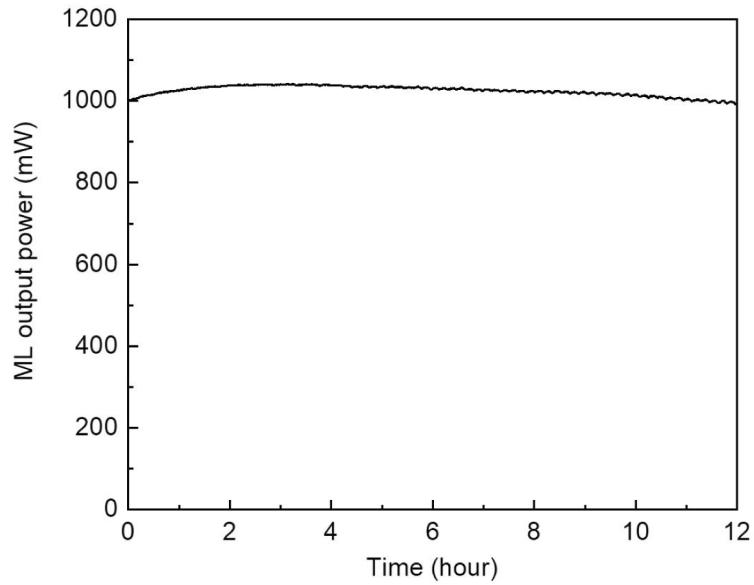


Fig. 5. Mode-locked output power stability over 12 h.

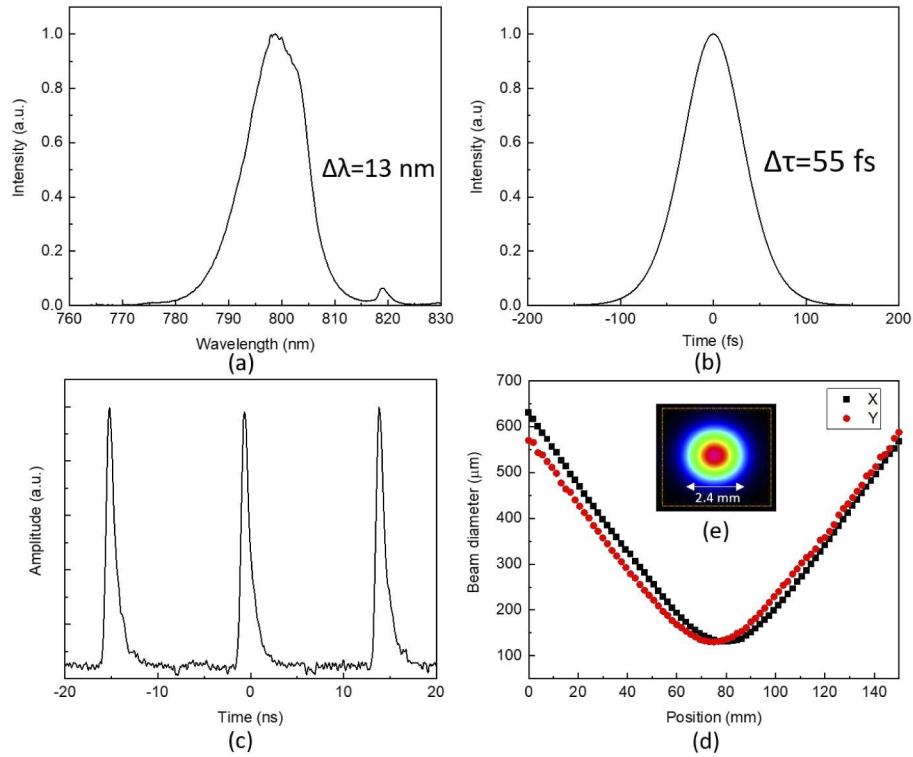


Fig. 6. (a) Measured output spectrum, (b) corresponding intensity autocorrelation, (c) pulse train, (d) M^2 value, and (e) inset: output beam profile.

4. Conclusion

We present the highest reported ML output power (W-class) from a self-starting Ti:S femtosecond laser using three spectrally combined pump diodes, which comprises aspheric lenses in the fast-axis direction and a shared simple cylindrical telescope in the slow-axis direction. The laser generated 1 W of ML average power and self-starting soliton-like pulses with 55 fs pulse durations at 68.8 MHz. This compact Ti:S laser is not only simple, robust, and inexpensive compared with a DPSSL-pumped laser but also capable of further power scaling through efficient pumping by focused circular beam owing to the different M^2 values of the diodes. Such reliable high-power and self-ML femtosecond pulses are very attractive for ultrafast applications. The proposed laser will be improved in future work to enhance the power output using both-way diode pumping. This pumping technique can also be applied to high-power Kerr-lens ML Ti:S lasers with short pulse less than 10 fs.

Note: A patent on this laser system is pending.

Funding. Electronics and Telecommunications Research Institute (21YR1800, 21YR2400).

Acknowledgments. The authors thank Eero Kiovusalo (RefleKron) for supplying SESAMs.

Disclosures. The authors declare no conflicts of interest.

Data availability. Data underlying the results presented in this paper are not publicly available but may be obtained from the corresponding author upon reasonable request.

References

1. P. F. Moulton, "Spectroscopic and laser characteristics of Ti:Sapphire ," *J. Opt. Soc. Am. B* **3**(1), 125–133 (1986).
2. I. B. Sohn, M. S. Lee, and S. M. Lee, "Femtosecond laser application to plc optical devices and packaging," *ETRI J* **27**(4), 446–448 (2005).
3. W. Denk, J. Strickler, and W. W. Webb, "Two-photon laser scanning fluorescence microscopy," *Science* **248**(4951), 73–76 (1990).
4. H. K. Soong and J. B. Malta, "Femtosecond lasers in ophthalmology," *Am. J. Ophthalmol.* **147**(2), 189–197.e2 (2009).
5. J. Doussot, G. Karras, F. Billard, P. Bejot, and O. Faucher, "Resonantly enhanced filamentation in gases," *Optica* **4**(7), 764–769 (2017).
6. T. Ideguchi, T. Nakamura, Y. Kobayashi, and K. Goda, "Kerr-lens mode-locked bidirectional dual-comb ring laser for broadband dual-comb spectroscopy," *Optica* **3**(7), 748–753 (2016).
7. T. Südmeyer, S. V. Marchese, S. Hashimoto, C. R. E. Baer, G. Gingras, B. Witzel, and U. Keller, "High-power ultrafast thin disk laser oscillators and their potential for sub-100-femtosecond pulse generation," *Nat. Photonics* **2**(10), 599–604 (2008).
8. D. H. Song, W. B. Cho, H. W. Lee, D. H. Shin, D.-K. Ko, and M. Y. Jung, "A compact kerr-lens mode-locked Ti:Sapphire oscillator with 330 nj soliton-like pulses," *Laser Phys. Lett.* **10**(6), 065003 (2013).
9. P. W. Roth, A. J. Maclean, D. Burns, and A. J. Kemp, "Direct diode-laser pumping of a mode-locked Ti:Sapphire laser," *Opt. Lett.* **36**(2), 304–306 (2011).
10. P. W. Roth, D. Burns, and A. J. Kemp, "Power scaling of a directly diode-laser-pumped Ti:Sapphire laser," *Opt. Express* **20**(18), 20629–20634 (2012).
11. C. G. Durfee, T. Storz, J. Garlick, S. Hill, J. A. Squier, M. Kirchner, G. Taft, K. Shea, H. Kapteyn, M. Murnane, and S. Backus, "Direct diode-pumped kerr-lens mode-locked Ti:Sapphire laser," *Opt. Express* **20**(13), 13677–13683 (2012).
12. K. Gürel, V. J. Wittwer, M. Hoffmann, C. J. Saraceno, S. Hakobyan, B. Resan, A. Rohrbacher, K. Weingarten, S. Schilt, and T. Südmeyer, "Green-diode-pumped femtosecond Ti:Sapphire laser with up to 450 mw average power," *Opt. Express* **23**(23), 30043–30048 (2015).
13. S. Backus, M. Kirchner, C. Durfee, M. Murnane, and H. Kapteyn, "Direct diode pumped Ti:Sapphire ultrafast regenerative amplifier system," *Opt. Express* **25**(11), 12469–12477 (2017).
14. J. C. E. Coyle, A. J. Kemp, J.-M. Hopkins, and A. A. Lagatsky, "Ultrafast diode-pumped Ti:Sapphire laser with broad tunability," *Opt. Express* **26**(6), 6826–6832 (2018).
15. F. X. Kärtner, I. D. Jung, and U. Keller, "Soliton mode-locking with saturable absorbers," *IEEE J. Sel. Top. Quantum Electron.* **2**(3), 540–556 (1996).
16. F. X. Kärtner, J. A. der Au, and U. Keller, "Mode-locking with slow and fast saturable absorbers-what's the difference?" *IEEE J. Sel. Top. Quantum Electron.* **4**(2), 159–168 (1998).
17. U. Keller, K. J. Weingarten, F. X. Kärtner, D. Kopf, B. Braun, I. D. Jung, R. Fluck, C. Honninger, N. Matuschek, and J. A. der Au, "Semiconductor saturable absorber mirrors (sesam's) for femtosecond to nanosecond pulse generation in solid-state lasers," *IEEE J. Sel. Top. Quantum Electron.* **2**(3), 435–453 (1996).

18. U. Keller, "Ultrafast solid-state laser oscillators: a success story for the last 20 years with no end in sight," *Appl. Phys. B* **100**(1), 15–28 (2010).
19. P. W. Roth, A. J. Maclean, D. Burns, and A. J. Kemp, "Directly diode-laser-pumped ti:sapphire laser," *Opt. Lett.* **34**(21), 3334–3336 (2009).
20. R. Sawada, H. Tanaka, N. Sugiyama, and F. Kannari, "Wavelength-multiplexed pumping with 478- and 520-nm indium gallium nitride laser diodes for ti:sapphire laser," *Appl. Opt.* **56**(6), 1654–1661 (2017).